

## Synthesis and Characterization of Novel “3 + 2” Oxorhenium Complexes, ReO[SNO][NN]

Aris Chiotellis,<sup>†,||</sup> Charalambos Tsoukalas,<sup>†</sup> Maria Pelecanou,<sup>‡</sup> Apostolos Papadopoulos,<sup>†</sup> Catherine Raptopoulou,<sup>§</sup> Aris Terzis,<sup>§</sup> Ioannis Pirmettis,<sup>†</sup> Minas Papadopoulos,<sup>\*,†</sup> and Efstratios Chiotellis<sup>||</sup>

*Institute of Radioisotopes–Radiodiagnostic Products, Institute of Biology, and Institute of Materials Science, National Centre for Scientific Research “Demokritos”, 15310 Athens, Greece, and School of Pharmacy, Aristotelian University of Thessaloniki, 54006 Thessaloniki, Greece*

Received March 13, 2006

The present paper deals with the synthesis and structural characterization of novel neutral oxorhenium(V) complexes of the general formula ReO[SNO][NN]. The simultaneous action of the tridentate SNO ligand, *N*-(2-mercaptoacetyl)-glycine (**1**), and the bidentate NN ligand, *N*-phenylpyridine-2-alimine (**2**), on ReOCl<sub>3</sub>(PPh<sub>3</sub>)<sub>2</sub> leads to the formation of two isomers **4a** and **4b** of the general formula ReO[SNO][NN], as a result of the different orientations of the NN ligand. In both cases, the SNO donor atoms of the tridentate ligand occupy the three positions in the equatorial plane of the distorted octahedron, whereas the oxo group is always directed toward one of the apical positions. In the first isomer, **4a**, the imino nitrogen of the NN ligand occupies the fourth equatorial position and the pyridine type nitrogen is directed trans to the oxo group, while in the second isomer, **4b**, the imino nitrogen of the NN ligand occupies the apical position trans to the oxo group and the pyridine type nitrogen completes the equatorial plane of the distorted octahedron. The [SNO][NN] mixed-ligand system was applied in the synthesis of the oxorhenium complex **5** in which the 1-(2-methoxyphenyl)piperazine moiety, a fragment of the true 5-HT<sub>1A</sub> antagonist WAY 100635, has been incorporated in the NN bidentate ligand (NN is *N*-{3-[4-(2-methoxyphenyl)piperazin-1-yl]propyl}-pyridine-2-alimine). In this case, high-performance liquid chromatography and NMR showed the existence of one isomer, **5**, in which the pyridine nitrogen is trans to the oxo core, as demonstrated by crystal structure analysis.

### Introduction

In the past 2 decades, the coordination chemistry of the group VII metals technetium and rhenium has been extensively investigated because of the widespread use of the metastable isotope <sup>99m</sup>Tc (pure  $\gamma$ -emitter, with ideal properties for imaging:  $t_{1/2} = 6$  h;  $E_{\gamma} = 140$  keV) in diagnostic nuclear medicine.<sup>1</sup> The introduction of the high-energy  $\beta$ -emitters <sup>186</sup>Re ( $t_{1/2} = 3.8$  days;  $E_{\max} = 1.07$  MeV) and

<sup>188</sup>Re ( $t_{1/2} = 0.7$  days;  $E_{\max} = 2.12$  MeV) in the development of therapeutic radiopharmaceuticals has made coordination studies on technetium and rhenium even more attractive.<sup>2</sup> Because of their similar chemical properties,<sup>1,2</sup> technetium and rhenium are considered a “matched pair” for tumor diagnosis and therapy because an existing <sup>99m</sup>Tc radiopharmaceutical, which accumulates in cancerous tissue, can be used as a model for the development of a <sup>186/188</sup>Re analogue aiming at targeted radiotherapy. Macroscopic-level inorganic chemistry of potentially useful complexes in nuclear medicine is commonly carried out by employing the “cold” natural isotopic mixture of <sup>185</sup>Re and <sup>187</sup>Re and, subsequently, transferring the chemistry at the tracer level (<sup>99m</sup>Tc and <sup>186/188</sup>Re).

New ligand systems for technetium and rhenium are continuously emerging, aiming at higher in vivo stability and

\* To whom correspondence should be addressed. E-mail: mspap@rrp.demokritos.gr. Tel.: +30210 6503909. Fax: +30210 6524 480.

<sup>†</sup> Institute of Radioisotopes–Radiodiagnostic Products, National Centre for Scientific Research “Demokritos”.

<sup>‡</sup> Institute of Biology, National Centre for Scientific Research “Demokritos”.

<sup>§</sup> Institute of Materials Science, National Centre for Scientific Research “Demokritos”.

<sup>||</sup> Aristotelian University of Thessaloniki.

(1) (a) Jurisson, S.; Berning, D.; Wei, J.; Ma, D. *Chem. Rev.* **1993**, *93*, 1137–1156. (b) Dilworth, J. R.; Parrott, S. *J. Chem. Soc. Rev.* **1998**, *27*, 43–55. (c) Jurisson, S. S.; Lydon, J. D. *Chem. Rev.* **1999**, *99*, 2205–2218. (d) Liu, S.; Edwards, D. S. *Chem. Rev.* **1999**, *99*, 2235–2268.

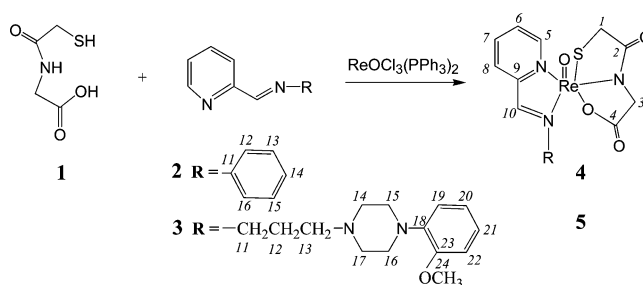
(2) (a) Volkert, W. A.; Hoffman, T. *J. Chem. Rev.* **1999**, *99*, 2269–2292. (b) Schubiger, P. A.; Alberto, R.; Smith, A. *Bioconjugate Chem.* **1996**, *7*, 165–179. (c) Reubi, J. C. *J. Nucl. Med.* **1995**, *36*, 1825.

improved pharmacokinetic properties of the complexes. Furthermore, the worldwide quest for site-specific radiopharmaceuticals requires that the ligating framework be easily derivatized for the incorporation of the biologically active molecule that will render specificity to the complex. The oxotechnetium  $\text{TcO}(\text{V})^{3+}$  and oxorhenium  $\text{ReO}(\text{V})^{3+}$  cores hold a prevalent role in the technetium and rhenium chemistry because many of the radiopharmaceuticals in clinical use today display a multidentate ligand wrapped around the oxometal core.<sup>1–3</sup>

A major class of oxotechnetium and oxorhenium complexes employs  $\text{N}_x\text{S}_{4-x}$  linear tetradentate ligands, like  $\text{N}_4$  propyleneamine oximes,<sup>4</sup>  $\text{N}_3\text{S}$  triamidomonothiols,<sup>5</sup>  $\text{N}_2\text{S}_2$  diamidodithiols,<sup>6</sup> monoamidomonoaminodithiols,<sup>7</sup> and diamidodithiols<sup>8</sup> that produce neutral, pentacoordinated complexes with square-pyramidal geometry. Another class for the synthesis of neutral oxometal(V) complexes involves the more flexible “3 + 1” donor atom system,<sup>9</sup> in which a combination of tridentate and monodentate ligands allows, in principle, the fine-tuning of the biological properties of the complexes through the selection of proper substituents. This approach has produced a series of pentacoordinated square-pyramidal or trigonal-bipyramidal complexes as potential brain radiopharmaceuticals. The drawback to the further development of the “3 + 1” class is its susceptibility to substitution reactions in vivo.<sup>10</sup> To alleviate such handicaps and increase stability, recent efforts have been focusing on the design of the “3 + 2” complexes in which a tridentate and a bidentate ligand (NSN/PO, NNN/PO, SNN/PO, SNO/PO, ONN/PO, ONO/PO, ONO/ON, and SNO/SN) coordinate with the oxometal(V) core to produce hexacoordinated, closed-shell, octahedral complexes.<sup>11</sup>

In the direction of designing small, neutral, and lipophilic model complexes for the development of receptor-based diagnostic and therapeutic radiopharmaceuticals, we have been investigating a novel “3 + 2” mixed-ligand system [SNO][NN], where SNO is a tridentate ligand amenable to deprotonation and NN is a bidentate Schiff base ligand

Scheme 1



originating from the reaction of 2-pyridinecarbaldehyde and a primary amine (Scheme 1).

In the initial step of this investigation, neutral, stable, hexacoordinated complexes of the  $\text{ReO}[\text{SNO}][\text{NN}]$  type (Scheme 1) were synthesized and structurally characterized employing *N*-(2-mercaptoacetyl)glycine (**1**) as the SNO tridentate ligand and two different NN Schiff base ligands, *N*-phenylpyridine-2-aldimine (**2**) and *N*-{3-[4-(2-methoxyphenyl)piperazin-1-yl]propyl}pyridine-2-aldimine (**3**). In **3**, the 1-(2-methoxyphenyl)piperazine moiety, a fragment of the true 5-HT<sub>1A</sub> antagonist WAY 100635,<sup>12</sup> has been incorporated. The major obvious advantage of this strategy is the fact that, through the use of different primary amines, tethering of a bioactive molecule to a stable neutral oxometal(V) complex can be easily achieved.

## Experimental Section

**Synthesis.** All chemicals were reagent-grade and were used without further purification. The SNO tridentate ligand, *N*-(2-mercaptoacetyl)glycine (**1**), was prepared by in situ deprotection of benzoyl(mercaptoacetyl)glycine.<sup>13</sup> The two bidentate ligands, *N*-phenylpyridine-2-aldimine<sup>14</sup> (**2**) and *N*-{3-[4-(2-methoxyphenyl)piperazin-1-yl]propyl}pyridine-2-aldimine<sup>15</sup> (**3**), were synthesized and purified according to published protocols (Scheme 1). Rhenium was purchased from Aldrich as  $\text{KReO}_4$  and was converted to the  $\text{ReOCl}_3(\text{PPh}_3)_2$  precursor as reported previously.<sup>16</sup> All compounds were characterized by IR and NMR spectroscopy. Solvents for high-performance liquid chromatography (HPLC) were

- (3) Johannsen, B.; Spies, H. *Top. Curr. Chem.* **1996**, *176*, 77–121.  
 (4) Jurisson, S.; Schlemper, E.; Troutner, D.; Canning, L.; Nowotnik, D.; Neirinx, R. *Inorg. Chem.* **1986**, *25*, 543–549.  
 (5) (a) Rao, T. N.; Adhikesavalu, D.; Camerman, A.; Fritzberg, A. R. *Inorg. Chim. Acta* **1991**, *180*, 63–67. (b) Guhlke, S.; Schaffland, A.; Zamora, P. O.; Sartor, J.; Diekmann, D.; Bender, H.; Knapp, F. F.; Biersack, H. J. *Nucl. Med. Biol.* **1998**, *25*, 621–631.  
 (6) Rao, T. N.; Adhikesavalu, D.; Camerman, A.; Fritzberg, A. R. *J. Am. Chem. Soc.* **1990**, *112*, 5798–5804.  
 (7) O’Neil, J. P.; Wilson, S. R.; Katzenellenbogen, J. A. *Inorg. Chem.* **1994**, *33*, 319–325.  
 (8) Meegalla, S.; Plossl, K.; Kung, M.-P.; Chumpradit, S.; Stevenson, D. A.; Kushner, S. A.; McElgin, W. T.; Mozley, P. D.; Kung, H. F. *J. Med. Chem.* **1997**, *40*, 9–17 and references cited therein.  
 (9) (a) Pietzsch, H.-J.; Spies, H.; Hoffmann, S.; Stach, J. *Inorg. Chim. Acta* **1989**, *161*, 15–16. (b) Mastrostamatis, S. G.; Papadopoulos, M. S.; Pirmettis, I. C.; Paschali, E.; Varvarigou, A. D.; Stassinopoulou, C. I.; Raptopoulou, C. P.; Terzis, A.; Chiotellis, E. *J. Med. Chem.* **1994**, *37*, 3212–3218. (c) Papadopoulos, M. S.; Pirmettis, I. C.; Pelecanou, M.; Raptopoulou, C. P.; Terzis, A.; Stassinopoulou, C. I.; Chiotellis, E. *Inorg. Chem.* **1996**, *35*, 7377–7383.  
 (10) (a) Pelecanou, M.; Pirmettis, I. C.; Nock, B. A.; Papadopoulos, M.; Chiotellis, E.; Stassinopoulou, C. I. *Inorg. Chim. Acta* **1998**, *281*, 148–152. (b) Syhre, R.; Seifert, S.; Spies, H.; Gupta, A.; Johannsen, B. *Eur. J. Nucl. Med.* **1998**, *25*, 793–796. (c) Nock, B.; Maina, T.; Yannoukakos, D.; Pirmettis, I. C.; Papadopoulos, M. S.; Chiotellis, E. *J. Med. Chem.* **1999**, *42*, 1066–1075.

- (11) (a) Nock, B.; Maina, T.; Tisato, F.; Papadopoulos, M.; Raptopoulou, C. P.; Terzis, A.; Chiotellis, E. *Inorg. Chem.* **1999**, *38*, 4197–4202. (b) Nock, B.; Maina, T.; Tisato, F.; Raptopoulou, C. P.; Terzis, A.; Chiotellis, E. *Inorg. Chem.* **2000**, *39*, 5197–5202. (c) Nock, B.; Maina, T.; Tisato, F.; Papadopoulos, M.; Raptopoulou, C. P.; Terzis, A.; Chiotellis, E. *Inorg. Chem.* **2000**, *39*, 2178–2184. (d) Melian, C.; Kremer, C.; Suescun, L.; Mombro, A.; Mariezcurrena, R.; Kremer, E. *Inorg. Chim. Acta* **2000**, *306*, 70–77. (e) Chen, X.; Femia, F. J.; Babich, J. W.; Zubieta, J. *Inorg. Chim. Acta* **2000**, *307*, 149–153. (f) Femia, F. J.; Chen, X.; Babich, J. W.; Zubieta, J. *Inorg. Chim. Acta* **2001**, *316*, 145–148. (g) Bolzati, C.; Porchia, M.; Bandoli, G.; Boschi, A.; Malago, E.; Uccelli, L. *Inorg. Chim. Acta* **2001**, *315*, 205–212. (h) Bereau, M. V.; Khan, I. S.; Abu-Omar, M. M. *Inorg. Chem.* **2001**, *40*, 6767–6773. (i) Mevellec, F.; Roucoux, A.; Noiret, N.; Patin, H. *Inorg. Chim. Acta* **2002**, *332*, 30–36.  
 (12) (a) Forster, E.; Cliffe, I.; Bill, D.; Dover, D.; Jones, G.; Reilly, Y.; Fletcher, A. *Eur. J. Pharmacol.* **1995**, *281*, 81–88. (b) Lang, L.; Jagoda, E.; Schmall, B.; Sassaman, M.; Ma, Y.; Eckelman, W. *Nucl. Med. Biol.* **2000**, *27*, 457–462.  
 (13) Schneider, R. F.; Subramanian, G.; Feld, T. A.; McAfee, J. G.; Zapf-Longo, C.; Palladino, E.; Thomas, F. D. *J. Nucl. Med.* **1984**, *25*, 223–229.  
 (14) (a) Johnson, D.; Mayer, H.; Minard, J.; Banaticla, J.; Miller, C. *Inorg. Chim. Acta* **1988**, *144*, 167–171. (b) Winn, M.; Dunnigan, D. A.; Zaugg, H. *J. Org. Chem.* **1968**, *33*, 2388–2392.  
 (15) Alberto, R.; Schibli, R.; Schubiger, A.; Abram, U.; Pietzsch, H.-J.; Johannsen, B. *J. Am. Chem. Soc.* **1999**, *121*, 6076–6077.  
 (16) Chatt, J.; Row, G. A. *J. Chem. Soc.* **1962**, 4019–4033.

HPLC-grade. They were filtered through membrane filters (0.22  $\mu\text{m}$ , Millipore, Milford, MA) and degassed by a helium flux before use.

IR spectra were recorded on KBr pellets on a Perkin-Elmer 1600 FT-IR spectrophotometer in the region 4000–500  $\text{cm}^{-1}$ . The NMR spectra were recorded in  $\text{CDCl}_3$  on a Bruker 500-MHz Avance DRX spectrometer using  $(\text{CH}_3)_4\text{Si}$  as the internal reference. Elemental analyses for C, H, N, and S were conducted on a Perkin-Elmer 2400/II automatic elemental analyzer. HPLC analysis was performed on a Waters 600E chromatography system coupled to a Waters 991 photodiode array detector. Separations were achieved on a Techsil C18 (10  $\mu\text{m}$ , 250 mm  $\times$  4 mm) column eluted with a binary gradient system at a 1.5  $\text{mL min}^{-1}$  flow rate. Mobile phase A was water containing 0.1% trifluoroacetic acid, while mobile phase B was methanol containing also 0.1% trifluoroacetic acid. The elution profile was 0–15 min to 30% B followed by a linear gradient to 40% in 5 min; this composition was held for another 10 min. After a column wash with 95% B for 5 min, the column was reequilibrated by applying the initial conditions (30% B) for 15 min prior to the next injection.

**ReO[SCH<sub>2</sub>CONCH<sub>2</sub>COO][*o*-C<sub>5</sub>H<sub>4</sub>NCH=NC<sub>6</sub>H<sub>5</sub>] (4).** To a solution of benzoyl(mercaptoacetyl)glycine (51 mg, 0.2 mmol) in 15 mL of methanol was added 1 mL of 1 M NaOH. The mixture was stirred for 30 min under nitrogen and then neutralized with 0.5 M HCl. To this solution were added under stirring  $\text{CH}_3\text{COONa}$  (164 mg, 2 mmol), **2** (34 mg, 0.2 mmol), and the precursor  $\text{ReOCl}_3\text{-(PPh}_3)_2$  (166.6 mg, 0.2 mmol). The mixture was refluxed until a clear solution formed (about 30 min). After the addition of  $\text{CH}_2\text{Cl}_2$ , the organic phase was washed with water, dried over  $\text{MgSO}_4$ , and concentrated to a small volume, and then 5 mL of methanol was added. Analysis of the solution by HPLC demonstrated the formation of two complexes, **4a** and **4b**, in a ratio of approximately 1:1. Slow evaporation of the solvents afforded a red-brown solid. Crystals suitable for X-ray studies were isolated by dissolving the precipitate in  $\text{CH}_2\text{Cl}_2/\text{MeOH}$  and allowing the solvent mixture to slowly evaporate. Through fractional crystallization, enrichment of the mixture in one of the complexes was possible; complete separation, however, of the two complexes was never achieved.

Yield: 70%. FT-IR ( $\text{cm}^{-1}$ , KBr pellet): 959, 970 ( $\text{Re}=\text{O}$ ). Anal. Calcd for  $\text{C}_{16}\text{H}_{14}\text{N}_3\text{O}_4\text{SRe}$ : C, 36.22; H, 2.66; N, 7.92; S, 12.06. Found: C, 36.30; H, 2.70; N, 7.85; S, 12.12.

**ReO[SCH<sub>2</sub>CONCH<sub>2</sub>COO][*o*-C<sub>5</sub>H<sub>4</sub>NCH=N(CH<sub>2</sub>)<sub>3</sub>N(CH<sub>2</sub>-CH<sub>2</sub>)<sub>2</sub>N-*o*-CH<sub>3</sub>OPh] (5).** The complex was synthesized and isolated in a similar manner using **3** (141 mg, 0.2 mmol) as the bidentate ligand. Analysis of the solution by HPLC demonstrated the formation of a single major product, **5**. The presence of a minor product (<5%) was also evident in the HPLC analysis. Crystals suitable for X-ray studies were isolated by dissolving the precipitate in  $\text{CH}_2\text{Cl}_2/\text{MeOH}$  and allowing the solvent mixture to slowly evaporate.

Yield: 72%. FT-IR ( $\text{cm}^{-1}$ , KBr pellet): 970 ( $\text{Re}=\text{O}$ ). Anal. Calcd for  $\text{C}_{24}\text{H}_{30}\text{N}_5\text{O}_5\text{SRe}$ : C, 41.97; H, 4.40; N, 10.20; S, 4.67. Found: C, 41.89; H, 4.50; N, 10.55; S, 4.57.

**X-ray Crystal Structure Determination of Complexes 4 and 5.** Crystals of compounds **4** and **5** suitable for X-ray analysis were mounted in air on a Crystal Logic Dual Goniometer diffractometer using graphite-monochromated Mo  $\text{K}\alpha$  radiation. Unit cell dimensions were determined by using the angular settings of 25 automatically centered reflections in the range  $11 < 2\theta < 23^\circ$ , and they appear in Table 1. Intensity data were recorded using a  $\theta$ - $2\theta$  scan. Three standard reflections monitored every 97 reflections showed less than 3% variation and no decay. Lorentz, polarization, and  $\psi$ -scan absorption corrections were applied using

**Table 1.** Summary of Crystal, Intensity Collection, and Refinement Data

	4	5
empirical formula	$\text{C}_{16}\text{H}_{14}\text{N}_3\text{O}_4\text{ReS}$	$\text{C}_{24}\text{H}_{30}\text{N}_5\text{O}_5\text{ReS}$
fw	530.56	686.79
temp (K)	298	298
wavelength ( $\lambda$ , Å)	Mo $\text{K}\alpha$ (0.710 730)	Mo $\text{K}\alpha$ (0.710 730)
space group	$P2_1/n$	$A2/n$
<i>a</i> (Å)	19.21(1)	14.269(6)
<i>b</i> (Å)	16.243(9)	10.548(5)
<i>c</i> (Å)	11.256(7)	33.90(2)
$\beta$ (deg)	107.34(2)	91.87(2)
<i>V</i> (Å <sup>3</sup> )	3352(3)	5099(4)
<i>Z</i>	8	8
<i>D</i> <sub>calcd</sub> ( $\text{Mg m}^{-3}$ )	2.102	1.789
abs coeff $\mu$ ( $\text{mm}^{-1}$ )	7.401	4.893
<i>F</i> (000)	2032	2720
GOF on <i>F</i> <sup>2</sup>	1.049	1.092
<i>R</i> indices	<i>R</i> 1 = 0.0459 <sup>a</sup> w <i>R</i> 2 = 0.1210 <sup>a</sup>	<i>R</i> 1 = 0.0379 <sup>b</sup> w <i>R</i> 2 = 0.0928 <sup>b</sup>

<sup>a</sup> For 5298 reflections with  $I > 2\sigma(I)$ . <sup>b</sup> For 3739 reflections with  $I > 2\sigma(I)$ .

Crystal Logic software. The structures were solved by direct methods using *SHELXS-86*<sup>17</sup> and refined by full-matrix least-squares techniques on *F*<sup>2</sup> using *SHELXL-97*.<sup>18</sup> Further crystallographic details for **4**:  $2\theta_{\text{max}} = 50^\circ$ , scan speed 4.2°  $\text{min}^{-1}$ , scan range 2.2 +  $\alpha_1\alpha_2$  separation, reflections collected/unique/used 7234/5889 [*R*<sub>int</sub> = 0.0716]/5889, 554 parameters refined,  $[\Delta\rho]_{\text{max}}/[\Delta\rho]_{\text{min}} = 0.920/-0.997 \text{ e } \text{Å}^{-3}$ ,  $[\Delta/\sigma]_{\text{max}} = 0.012$ , *R*1/w*R*2 (for all data) = 0.0508/0.1267. All hydrogen atoms were located by difference maps and were refined isotropically (except those on C13, C14, and C28, which were introduced at calculated positions as riding on bonded atoms); all non-hydrogen atoms were refined anisotropically. Further crystallographic details for **5**:  $2\theta_{\text{max}} = 50^\circ$ , scan speed 2.0°  $\text{min}^{-1}$ , scan range 2.2 +  $\alpha_1\alpha_2$  separation, reflections collected/unique/used 4567/4483 [*R*<sub>int</sub> = 0.0350]/4483, 433 parameters refined,  $[\Delta\rho]_{\text{max}}/[\Delta\rho]_{\text{min}} = 0.973/-0.993 \text{ e } \text{Å}^{-3}$ ,  $[\Delta/\sigma]_{\text{max}} = 0.004$ , *R*1/w*R*2 (for all data) = 0.0491/0.1022. All hydrogen atoms were located by difference maps and were refined isotropically (except those on C11, which were introduced at calculated positions as riding on bonded atoms); all non-hydrogen atoms were refined anisotropically.

## Results and Discussion

**Synthesis.** Reaction of equimolar amounts of the SNO tridentate ligand, **1**, and the NN bidentate ligand, **2**, with the  $\text{Re}^{\text{VOCl}}_3(\text{PPh}_3)_2$  precursor (Scheme 1) led to the formation of two complexes of **4** (**4a** and **4b**) in a ratio of approximately 1:1, as revealed by HPLC and NMR. Formation of isomeric complexes is theoretically possible because the bidentate NN ligand can approach the oxorhenium core in different ways. Indeed, X-ray analysis of the crystals isolated during synthesis revealed that in complex **4a** the pyridine nitrogen of the NN ligand is oriented trans to the oxometal group, while in complex **4b** the imine nitrogen of the NN ligand is oriented trans to the oxo core.

The Schiff base **3**, carrying the biologically active 1-(2-methoxyphenyl)piperazine moiety, which is a fragment of the true 5-HT<sub>1A</sub> antagonist WAY 100635, was subsequently employed as the NN bidentate ligand. Under the same

(17) Sheldrick, G. M. *SHELXS-86, Structure Solving Program*; University of Göttingen, Germany, 1986.

(18) Sheldrick, G. M. *SHELXL-97: Program for Crystal Structure Refinement*; University of Göttingen: Göttingen, Germany, 1997.

conditions as those above, HPLC analysis of the crude reaction mixture indicated the formation of a single compound **5** (>95%), in which the pyridine nitrogen of the NN ligand is positioned trans to the oxo core, as revealed by X-ray analysis. The existence of only one isomer in the reaction mixture was also evident in the NMR spectra.

Preferential formation of one stereoisomer over the other has been reported in the literature for other oxorhenium(V) and oxotechnetium(V)  $\text{MO}[\text{N}_2\text{S}_2]$  and  $\text{MO}[\text{SNS}][\text{S}]$  ( $\text{M} = \text{Tc}, \text{Re}$ ) complexes;<sup>19</sup> the factors, however, governing the observed stereoselectivity are not well understood. Apparently, a combination of steric and electronic parameters determine the way a ligand binds to the metal center. In complex **4**, the comparable sizes and similar chemical character of pyridine and the phenyl ring of the NN ligand **2** do not impose significant thermodynamic barriers on the way that **2** is positioned, and both isomers are formed. In the case of complex **5**, the size of the NN ligand **3** appears to be a significant factor in the preferential formation of the isomer in which the bulky *N*-3-[4-(2-methoxyphenyl)piperazin-1-yl]propyl side chain is directed away from the metal-coordination sphere and steric interactions with the SNO ligand are minimized. Alternative positioning of the NN ligand **3** trans to the oxometal center would limit to some extent the kinetic freedom of the side chain. The preference of the  $\text{sp}^2$  nitrogen donor atom of the NN bidentate ligand to occupy the apical position trans to the oxygen of the oxorhenium(V) core has been observed in all other monooxo octahedral oxorhenium and oxotechnetium  $\text{MO}[\text{NN}][\text{X}]_3$  complexes, with NN being 2,2'-bipyridine,<sup>20a,b</sup> biimidazole,<sup>20b</sup> 2-(2'-pyridyl)benzothiazole,<sup>20c,d</sup> 2-(2'-pyridyl)benzoxazole,<sup>20d</sup> or diazabutadienes<sup>20e</sup> and X being monodentate chlorine or thiophenol ligands.

The newly synthesized compounds were extracted in  $\text{CH}_2\text{Cl}_2$  and isolated as crystalline products from  $\text{CH}_2\text{Cl}_2/\text{MeOH}$ . All complexes gave correct elemental analyses and were characterized by IR and NMR spectroscopy and X-ray crystallography. They are soluble in  $\text{CH}_2\text{Cl}_2$  and chloroform, slightly soluble in methanol or ethanol, and insoluble in ether, pentane, and water. They are stable in the solid state as well as in organic solutions (for a period of months), as shown by HPLC and NMR. Their stability is not affected by the presence of air or moisture.

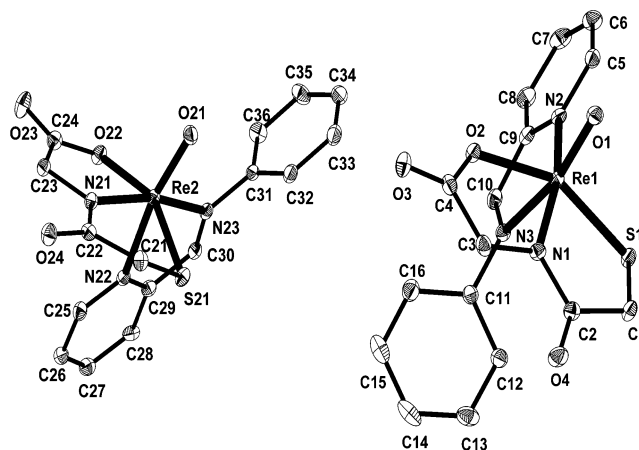


**Figure 1.** Labeled ORTEP diagram showing both isomers, **4a** (left) and **4b** (right), with thermal ellipsoids drawn at 40% probability. Hydrogen atoms have been omitted for clarity.

**Table 2.** Selected Bond Distances (Å) and Angles (deg) for **4a** and **4b**

4a		4b	
Distances			
Re2—O21	1.690(6)	Re1—O1	1.678(6)
Re2—N21	1.973(6)	Re1—N1	1.977(6)
Re2—O22	2.049(6)	Re1—O2	2.048(5)
Re2—N23	2.146(7)	Re1—N3	2.261(6)
Re2—N22	2.267(7)	Re1—N2	2.180(6)
Re2—S21	2.308(2)	Re1—S1	2.304(2)
Angles			
O21—Re2—N21	108.7(3)	O1—Re1—N1	108.6(3)
O21—Re2—O22	101.4(3)	O1—Re1—O2	101.8(3)
N21—Re2—O22	79.1(2)	N1—Re1—O2	78.8(2)
O21—Re2—N23	88.2(3)	O1—Re1—N2	88.0(3)
N21—Re2—N23	162.2(3)	N2—Re1—N1	162.8(2)
O22—Re2—N23	92.3(2)	O2—Re1—N2	93.8(2)
O21—Re2—N22	159.0(3)	O1—Re1—N3	158.1(2)
N21—Re2—N22	91.6(2)	N1—Re1—N3	92.4(2)
O22—Re2—N22	76.3(2)	O2—Re1—N3	75.6(2)
N23—Re2—N22	71.2(2)	N2—Re1—N3	70.6(2)
O21—Re2—S21	103.0(2)	O1—Re1—S1	103.3(2)
N21—Re2—S21	82.9(2)	N1—Re1—S1	83.3(2)
O22—Re2—S21	153.2(2)	O2—Re1—S1	153.2(2)
N23—Re2—S21	99.2(2)	N2—Re1—S1	96.4(2)
N22—Re2—S21	98.3(3)	N3—Re1—S1	84.5(2)

The IR spectrum of **4** (a mixture of **4a** and **4b**) exhibits, as expected, two oxorhenium characteristic stretching bands that were specifically assigned (**4a** at  $970\text{ cm}^{-1}$  and **4b** at  $959\text{ cm}^{-1}$ ) by comparison of their relative intensities to the analogy of the isomers in the NMR spectrum of the mixture. The oxorhenium stretching band of **5** appears at  $970\text{ cm}^{-1}$ . These values are consistent with those reported for several other well-characterized monooxo complexes of rhenium.<sup>11</sup>

**X-ray Crystallography.** Compound **4** crystallizes in the monoclinic space group  $P2_1/n$  with two crystallographically independent molecules in the asymmetric unit (**4a** and **4b**). The molecular structures of both molecules are given in Figure 1, and selected bond distances and angles are listed in Table 2. Compound **5** crystallizes in the monoclinic space group  $A2/n$  with one crystallographically independent molecule in the asymmetric unit. The molecular structure of **5** is shown in Figure 2, and selected bond distances and angles are given in Table 3. In all complexes, the coordination geometry around the rhenium is distorted octahedral comprised by the SNO donor atom set of the tridentate ligand,

- (19) (a) Hansen, L.; Lipowska, M.; Meléndez, E.; Xu, X.; Hirota, S.; Taylor, A. T.; Marzilli, L. G. *Inorg. Chem.* **1999**, *38*, 5351–5358. (b) Marzilli, L. G.; Banaszczyk, M. G.; Hansen, L.; Kuklennyk, Z.; Cini, R.; Taylor, A., Jr. *Inorg. Chem.* **1994**, *33*, 4850–4860. (c) Mahmood, A.; Baidoo, K. E.; Lever, S. Z. In *Technetium and Rhenium in Chemistry and Nuclear Medicine 3*; Nicolini, M., Bandoli, G., Mazzi, U., Eds.; Cortina International: Verona, Italy, 1990; pp 119–124. (d) Papadopoulos, M.; Pirmettis, I.; Pelecanou, M.; Raptopoulou, C. P.; Terzis, A.; Stassinopoulou, C. I.; Chiotellis, E. *Inorg. Chem.* **1996**, *35*, 7377.
- (20) (a) Papachristou, M.; Pirmettis, I. C.; Tsoukalas, Ch.; Papagiannopoulou, D.; Raptopoulou, C.; Terzis, A.; Stassinopoulou, C. I.; Chiotellis, E.; Pelecanou, M.; Papadopoulos, M. *Inorg. Chem.* **2003**, *42*, 5778–5784. (b) Fortin, S.; Beauchamp, A. L. *Inorg. Chem.* **2000**, *39*, 4886–4893. (c) Tzanopoulou, S.; Pirmettis, I. C.; Patsis, G.; Raptopoulou, C.; Terzis, A.; Papadopoulos, M.; Pelecanou, M. *Inorg. Chem.* **2006**, *45*, 902–909. (d) Gangopadhyay, J.; Sengupta, S.; Bhattacharyya, S.; Chakraborty, I.; Chakravorty, A. *Inorg. Chem.* **2002**, *41*, 2616–2622. (e) Das, S.; Chakraborty, I.; Chakravorty, A. *Inorg. Chem.* **2003**, *42*, 6545–6555.

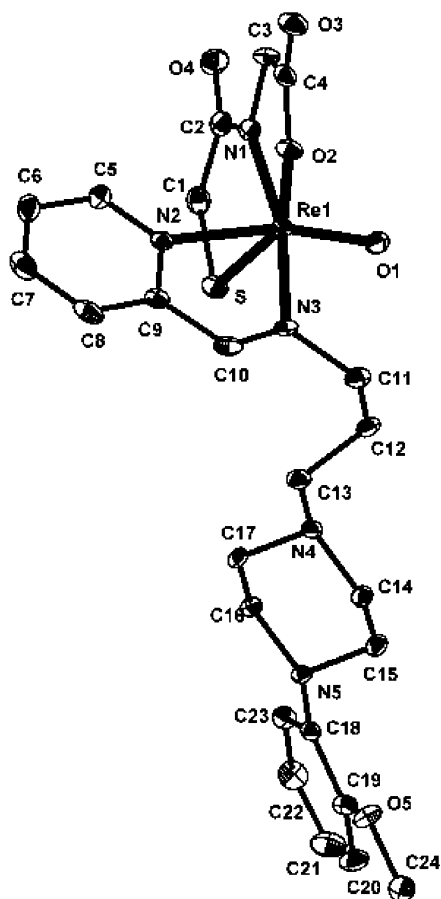


**Figure 2.** Labeled ORTEP diagram of **5** with thermal ellipsoids drawn at 40% probability. Hydrogen atoms have been omitted for clarity.

**Table 3.** Selected Bond Distances (Å) and Angles (deg) for **5**

Distances			
Re1–O1	1.670(5)	Re1–N3	2.127(6)
Re1–N1	1.967(6)	Re1–N2	2.281(6)
Re1–O2	2.058(5)	Re1–S	2.299(2)
Angles			
O1–Re1–N1	107.2(3)	O2–Re1–N2	76.9(2)
O1–Re1–O2	102.2(2)	N2–Re1–N3	71.5(2)
N1–Re1–O2	79.2(2)	O1–Re1–S	104.1(2)
O1–Re1–N3	89.2(3)	N1–Re1–S	83.7(2)
N1–Re1–N3	163.0(2)	O2–Re1–S	151.9(2)
O2–Re1–N3	93.0(2)	N3–Re1–S	97.1(2)
O1–Re1–N2	160.5(3)	N2–Re1–S	81.5(2)
N1–Re1–N2	91.8(2)		

the two nitrogen atoms of the bidentate ligand, and the double-bonded oxygen atom. In all cases, the SNO donor atoms of the tridentate ligand occupy three positions in the equatorial plane of the distorted octahedron, whereas the oxo group is always directed to one of the apical positions. Depending on the way that the NN bidentate ligand approaches rhenium, we identify two isomers: in the first isomer, **4a**, the pyridine type nitrogen of the NN ligand is directed trans to the oxo group and the imino nitrogen occupies the fourth equatorial position, while in the second isomer, **4b**, the imino nitrogen of the NN ligand occupies the apical position trans to the oxo group and the pyridine type nitrogen completes the equatorial plane of the distorted octahedron. The crystal structure of complex **5** shows that the pyridine type nitrogen of the NN ligand is directed trans

to the oxo group, as is the case of **4a**. The presence of isomers **4a** and **4b** as two crystallographically independent molecules in the same asymmetric unit is particularly interesting and suggests that both isomers can be equally "frozen" in the solid state. The oxo group exerts significant trans influence to the Re–N(pyridine) and Re–N(imine) bond lengths in both isomers. In particular, in isomers **4a** and **5**, where the pyridine type nitrogen is trans to the oxo group, the Re–N(pyridine) bond distances [2.267(7) Å in **4a** and 2.281(6) Å in **5**] are longer than the Re–N(pyridine) distance [2.180(6) Å] in **4b**, where the imine type nitrogen is trans to the oxo group. In addition, the Re–N(imine) bond distances are longer [2.261(6) Å] in **4b** than in **4a** [2.146(7) Å] and **5** [2.127(6) Å]. In all cases, rhenium lies above the equatorial plane of the distorted octahedron toward the doubly bonded oxygen atom (0.36, 0.37, and 0.38 Å for **4a**, **4b**, and **5**, respectively). The Re=O axis is inclined at 79.6, 79.3, and 80.5° with respect to the equatorial plane of the octahedron in **4a**, **4b**, and **5**, respectively. There are three five-membered chelating rings in the coordination sphere. The one defined by the Re–N–C–C–O atoms of the tridentate ligand and the second defined by the Re–N–C–C–N atoms of the bidentate ligand are planar. The third five-membered chelating ring, defined by the Re–S–C–C–N atoms of the tridentate ligand, adopts in all complexes the envelope configuration, with the sulfur atom displaced out of the mean plane of the remaining four atoms (0.64, 0.54, and 0.26 Å in **4a**, **4b**, and **5**, respectively). The angles around rhenium within the tetragonal plane of the octahedron range from 79.1(2) to 99.2(2)° (in **4a**), from 78.8(2) to 96.4(2)° (in **4b**), and from 79.2(2) to 97.1(2)° (in **5**), whereas those involving the apical atoms range from 71.2(2) to 108.7(3)° (in **4a**), from 70.6(2) to 108.6(3)° (in **4b**), and from 71.5(2) to 107.2(3)° (in **5**). As expected, the bite angle of the bidentate ligand (N–Re–N) is the smallest one in the coordination sphere. All bonding distances in the coordination sphere fall in the ranges observed in analogous complexes.

**NMR Studies.** <sup>1</sup>H and <sup>13</sup>C NMR chemical shift assignments for complexes **4** and **5** were based on the combined analysis of <sup>1</sup>H–<sup>1</sup>H and <sup>1</sup>H–<sup>13</sup>C correlation spectra and are reported in Table 4. The numbering of the atoms is shown in Scheme 1.

In the case of complex **4**, two entities of similar but distinct structure, each bearing **2** (NN ligand) and **1** (SNO ligand), were present in solution. Their spectra were in agreement with the isomeric structures resulting from the different positioning of the ligand with respect to the oxorhenium core, as revealed by the X-ray crystallographic analysis (Figure 1). No interconversion between the isomers was noted during the NMR studies. Distinction of the chemical shifts of each isomer was based on the presence of nuclear Overhauser effect (nOe) peaks. Specifically, isomer **4a**, where the pyridine nitrogen is coordinated trans to the oxo group, is characterized by nOe interaction peaks between the H1 and H3 methylene protons of the SNO ligand and the H5 proton of the pyridine moiety. On the other hand, isomer **4b**, where the imine nitrogen is coordinated trans to the oxo group, is

**Table 4.**  $^1\text{H}$  and  $^{13}\text{C}$  NMR Chemical Shifts (ppm) for Complexes **4a**, **4b**, and **5** in  $\text{CDCl}_3$  at 25 °C

	<b>4a</b>	<b>4b</b>		<b>4a</b>	<b>4b</b>	<b>5</b>			
H1	4.71, 3.88	4.63, 3.68	C1	45.76	45.89	H1	4.66, 3.88	C1	46.07
H3	4.66	4.29, 3.41	C2	189.12	188.68	H3	4.67	C2	188.91
H5	7.91	9.38	C3	55.58	55.08	H5	7.80	C3	55.41
H6	7.23	7.72	C4	186.25	187.03	H6	7.17	C4	186.48
H7	7.99	7.94	C5	147.80	151.88	H7	7.92	C5	147.67
H8	7.81	8.11	C6	127.53	126.27	H8	7.68	C6	127.16
H10	8.29	8.39	C7	138.74	140.92	H10	8.48	C7	138.81
H12/H16	7.69	7.02	C8	129.20	128.19	H11	4.60, 4.52	C8	128.10
H13/H15	7.51	7.37	C9	151.22	151.74	H12	2.50	C9	152.48
H14	7.51	7.35	C10	162.16	159.70	H13	2.62	C10	162.25
			C11	154.60	146.58	H14/H17	2.72, 2.65	C11	66.72
			C12/C16	122.15	121.62	H15/H16	3.12	C12	22.66
			C13/C15	129.31	129.45	H20	6.87	C13	54.65
			C14	129.31	129.45	H21	7.01	C14/C17	53.21
						H22	6.94	C15/C16	50.43
						H23	6.94	C18	140.91
						H24	3.87	C19	152.58
								C20	111.34
								C21	123.22
								C22	121.02
								C23	118.20
								C24	55.52

characterized by nOe peaks between the H1 and H3 methylene protons of the SNO ligand and the H12/H16 protons of the phenyl ring.

The most notable  $^1\text{H}$  NMR chemical shift difference between **4a** and **4b** is recorded for the H5 proton of the pyridine moiety, which appears deshielded by approximately 1.5 ppm in **4b** compared to **4a**. This difference may be attributed to the chemical shift anisotropy of the  $\text{Re}=\text{O}$  core that is known to differentially affect the chemical shifts of neighboring protons depending on their placement relative to the oxometal center.<sup>21</sup> It may also be partially due to the nonbonded interaction of H5 with the oxorhenium oxygen. According to the crystallographic data, the distance of H5 from the oxygen atom of the  $\text{Re}=\text{O}$  core in **4b** is 2.43 Å, a distance that may allow the distortion of the electron cloud of H5 by the more electronegative oxygen. For the corresponding C5 carbons, the chemical shift difference between **4b** and **4a** is 4 ppm.

Another interesting difference between **4a** and **4b** is noted for the H3 geminal protons of the SNO ligand backbone. In isomer **4b**, these protons are differentiated according to their orientation with respect to the oxorhenium core, with the endo (facing toward the oxygen of the  $\text{Re}=\text{O}$ ) being deshielded by 0.9 ppm compared to the exo (facing away from the oxygen of the  $\text{Re}=\text{O}$  core). In isomer **4a**, protons H3 have very similar chemical shifts and they appear as a multiplet centered at 4.66 ppm. The placement of the pyridine moiety trans to the oxometal core in **4a** appears to influence the appearance of H3 because undifferentiated H3 protons are also present in complex **5**, which has a configuration similar to that of **4a** with the pyridine moiety placed trans to the oxometal position.

Finally, the weakening of the  $\text{Re}-\text{N}(\text{imine})$  bond when positioned trans to the oxygen in isomer **4b** [Table 2;  $\text{Re}2-\text{N}23$  is 2.146(7) Å for isomer **4a** and  $\text{Re}1-\text{N}3$  is 2.261(6)

Å for isomer **4b**] is reflected in the chemical shift of the C11 quaternary carbon. Specifically, in **4b**, where the electron pull by the metal center is less effective, C11 appears shielded by 8 ppm compared to **4a**. The same argument applies to the effect of the length of the  $\text{Re}-\text{N}(\text{pyridine})$  bond on the chemical shift of C5. In **4b**, where the electron pull by the metal center is more effective [Table 2;  $\text{Re}2-\text{N}22$  is 2.267(7) Å for isomer **4a** and  $\text{Re}1-\text{N}2$  is 2.180(6) Å for isomer **4b**], C5 is deshielded by 4 ppm compared to **4a**.

In conclusion, in this work a novel “3 + 2” mixed-ligand system combining a SNO tridentate ligand and a NN bidentate ligand is introduced. This system leads to 18-electron octahedral  $[\text{SNO}][\text{NN}]$  neutral and stable oxorhenium complexes. Because the bidentate ligand is a Schiff base originating from the reaction of 2-pyridinecarbaldehyde and a primary amine, any bioactive molecule that carries a primary amine can, in principle, be incorporated in the NN bidentate ligand in order to render specificity to the complex. The successful formation of a “3 + 2” mixed-ligand complex carrying the bioactive moiety for 5-HT<sub>1A</sub> receptors exemplifies the potential of this system, which is currently being investigated in our laboratory through the use of a variety of small bioactive molecules. Transfer of the chemistry at technetium ( $^{99\text{m}}\text{Tc}$ ) and rhenium ( $^{186/188}\text{Re}$ ) tracer levels is also in course in order to investigate the applicability of this system for the development of potential radiopharmaceuticals.

**Acknowledgment.** This work was supported by the General Secretariat of Research and Technology (GSRT) of Greece (PENED01 1081).

**Supporting Information Available:** Crystallographic data in CIF format for the structures of the complexes **4a**, **4b**, and **5**. This material is available free of charge via the Internet at <http://pubs.acs.org>.

IC0604260

(21) Pelecanou, M.; Chryssou, K.; Stassinopoulou, C. I. *J. Inorg. Biochem.* **2000**, *79*, 347–351.